FTIR Spectroscopy Reveals Microscopic Structural Changes of the Protein around the Rhodopsin Chromophore upon Photoisomerization†

Hideki Kandori and Akio Maeda*

Department of Biophysics, Graduate School of Science, Kyoto University, Sakyo-ku, Kyoto 606-01, Japan

Received July 10, 1995; Revised Manuscript Received August 24, 1995⊗

ABSTRACT: Fourier transform infrared spectroscopy was used to investigate the local structure around the chromophore of rhodopsin and its change upon photoisomerization. A hydrated film of bovine rod outer segments was cooled at 80 K, and difference infrared spectra were obtained between bathorhodopsin and rhodopsin or between bathorhodopsin and isorhodopsin under suitable irradiation conditions. The spectra in a higher-frequency region (4000−1800 cm^{-1}) revealed protein structural change by probing the O−H, N−H, and S−H stretching vibrational modes. The structural change of bound water molecules occurred upon formation of bathorhodopsin, where three water O−H increased the strength of their H-bonding. The water structure is identical in rhodopsin and isorhodopsin. These results suggest that the protein in the close proximity of the Schiff base of the chromophore is perturbed upon photoisomerization and causes rearrangement of the water molecules in bathorhodopsin. Upon the isomerization, the 3463 cm^{-1} band of the 11-cis form (rhodopsin) shifts to 3487 cm^{-1} for the all-trans form (bathorhodopsin) or to 3481 cm^{-1} for the 9-cis form (isorhodopsin). An N−H bond, possibly of an indole of tryptophan residue, is responsible for these bands. It is present in a hydrophobic environment around the β-ionone ring and/or polyene chain of the retinal, and changes its geometrical alignment depending on the isomeric state. It is the only band distinct in frequency between rhodopsin and isorhodopsin in the high-frequency region, suggesting that the specific interaction between the N−H and the chromophore contributes to the more efficient isomerization in rhodopsin than isorhodopsin. The stretching vibrations of the water O−H, cysteine S−H, and amide N−H of the peptide backbone decrease in frequency upon formation of bathorhodopsin, indicating that H-bonding around the chromophore becomes stronger in bathorhodopsin. This shows that at least a part of the energy absorbed in the chromophore is already transferred to the protein in bathorhodopsin by strengthened H-bonding. The chromophore−protein interaction as a suitable reaction field in rhodopsin is discussed on the basis of these observations.

Rhodopsin is a photoreceptor protein present in the disk membranes of the rod outer segments (ROS)[1] of the retina. Light absorption by its chromophore, an 11-cis retinal bound to Lys296 (in case of bovine rhodopsin) through the protonated Schiff base, induces the cis−trans isomerization of the chromophore (Birge, 1990; Yoshizawa & Kandori, 1992). The chromophore−protein interaction appears to be designed so as to yield the protein structural changes by use of the acquired light energy, leading finally to the formation of a structure (called "metarhodopsin-II") to activate the GTP-binding protein, transducin (Stryer, 1991; Nathans, 1992). Since rhodopsin is easily purified from animal eyes and its function can be triggered by light, it is considered to be the most suitable system to investigate the signal transduction mechanism in G-protein-coupled receptors. Indeed, the specific rhodopsin−transducin interaction has been extensively studied by various spectroscopic, biochemical, and molecular biological methods (Emeris et al., 1982; König et al., 1989; Franke et al., 1990).

Regarding the rhodopsin molecule itself, elucidation of the relation between its structure and function has been of a central interest, namely, the determination of its tertiary structure and the understanding of the intramolecular signal transduction to activate transducin in terms of protein structure changes. The tertiary structure of rhodopsin has not been determined yet. Schertler et al. (1993) show the presence of seven transmembrane helices in bovine rhodopsin, but the resolution in their electron diffraction study has not yet reached an atomic level. However, the study of the structure of rhodopsin has yielded many promising results in the structure surrounding the chromophore. Since the rhodopsin chromophore is probed well by its visible absorption spectra, many studies for the modified chromophore or protein have been reported. In particular, site-directed mutagenesis has scored great success in studying chromophore−protein interaction. It revealed the Schiff base counterion to be Glu113 (Zhukovsky & Oprian, 1989; Sakmar et al., 1989; Nathans, 1990) or various amino acid residues whose substitutions significantly influence visible absorption spectrum [for a review, see Nathans (1992) and references therein]. Recently, vibrational spectroscopy of rhodopsin mutants such as resonance Raman (Lin et al., 1992) and Fourier transform infrared (FTIR) (Fahmy et al., 1993, 1994; Rath et al., 1993; Jäger et al., 1994) has been successfully applied to investigate local structure around the chromophore of rhodopsin.

† This work is supported by grants from the Japanese Ministry of Education, Culture and Science to A.M. (06404082) and to H.K. (07228231, 07839003).

* Correspondence should be addressed to this author. Department of Biophysics, Graduate School of Science, Kyoto University, Sakyo-ku, Kyoto 606-01, Japan. Tel./Fax: +81-75-753-4210.

⊗ Abstract published in *Advance ACS Abstracts,* October 1, 1995.

[1] Abbreviations: ROS, rod outer segments; FTIR, Fourier transform infrared; HOOP, hydrogen out-of-plane vibration; B/R, bathorhodopsin minus rhodopsin; B/I, bathorhodopsin minus isorhodopsin; I/R, isorhodopsin minus rhodopsin.

0006-2960/95/0434-14220$09.00/0

Visible spectroscopy, either as steady-state spectra at low temperatures or in a time-resolved manner at ambient temperatures (Shichida, 1986), has revealed that the photochemical process of rhodopsin is composed of the sequential intermediate states, photorhodopsin, bathorhodopsin, lumirhodopsin, metarhodopsin-I, and metarhodopsin-II. One of interesting issues regarding the photochemical processes concerns the first stage, the mechanisms of highly efficient photoisomerization of the chromophore and energy storage in bathorhodopsin. The highly efficient photoisomerization of rhodopsin (the quantum yield is 0.67; Dartnall, 1967) is assured by the extremely fast cis−trans isomerization of the chromophore (Schoenlein et al., 1991; Wang et al., 1994). The lower quantum yield of the corresponding protonated Schiff base in solution (~0.2; Becker & Freedman, 1985; Koyama et al., 1991) implies a contribution of the protein moiety in the isomerization process of rhodopsin. Several theoretical approaches have been performed to explain the efficient isomerization in the protein (Warshel, 1976; Liu & Asato, 1985; Warshel et al., 1991; Tallent et al., 1992; Kakitani et al., 1992). Similarly, the lower quantum yield of isorhodopsin (9-cis rhodopsin) suggests that the protein structure of rhodopsin is more favorable for the efficient isomerization than that of isorhodopsin (Kropf & Hubbard, 1958; Kandori et al., 1988). Comparisons of the protein structures between rhodopsin and isorhodopsin are thus of important.

The rapid isomerization thereby leads to the formation of the primary intermediates, such as photorhodopsin (Shichida et al., 1984; Kandori et al., 1989b) or bathorhodopsin (Yoshizawa & Wald, 1963; Kandori et al., 1989b), in high-energy states. Earlier resonance Raman spectroscopy of bathorhodopsin revealed the distorted structure of the chromophore through the analysis of the hydrogen out-of-plane (HOOP) vibrational modes (Eyring et al., 1982; Palings et al., 1989). It could constitute one of the modes for light energy storage in bathorhodopsin (~35 kcal/mol; Cooper, 1979). Additional secrets of the efficient isomerization and energy storage will be hidden in the other structural features of bathorhodopsin.

FTIR spectroscopy is a powerful tool for probing the protein structure as well as the chromophore structure (Maeda, 1995). The FTIR spectra of the photolyzed rhodopsin in the lower-frequency region (1800−800 cm^{-1}) have been recorded (Siebert et al., 1983; Bagley et al., 1985; DeGrip et al., 1988). We have now measured the difference FTIR spectra among rhodopsin, bathorhodopsin, and isorhodopsin at 80 K in the whole mid-infrared region (4000−800 cm^{-1}). The improved equipment used in the present study could limit the fluctuation within an order of 10^{-4} absorbance unit in the whole region. Furthermore, several repeated recordings allowed the detection of absorbance changes as small as 10^{-5}. Such technical advances in recording infrared spectral changes in the 4000−1800 cm^{-1} region have opened the way to resolve the structural change of the rhodopsin molecule in more detail, particularly from the protein side.

The FTIR difference spectra that probed the O−H, S−H, and N−H vibrations revealed changes in (i) the structure of water, (ii) the structure of cysteine S−H, (iii) the structure of peptide N−H, and (iv) the specific interaction of the chromophore with free and D_2O-insensitive N−H, which is most likely to be an indole N−H of a tryptophan residue, upon formation of bathorhodopsin. The results i−iii show that H-bonding of these bonds becomes stronger in bathorhodopsin. By postulating that the protein structural change detected among rhodopsin, bathorhodopsin, and isorhodopsin is limited around the chromophore, we argue for specific chromophore−protein interactions in relation to these functional bonds.

MATERIALS AND METHODS

Bovine ROS were isolated by flotation on a discontinuous sucrose gradient (Kandori et al., 1989a). ROS were washed three times with 10 mM Hepes buffer (pH 7.0) by centrifugation at 55 000*g* and then suspended in 10 mM Hepes buffer containing 50 mM hydroxylamine (pH 7.0) to convert the retinals contained in the ROS to the oximes. The ROS were washed five times with 10 mM Hepes buffer and finally three times with distilled water.

A 40 μL aliquot of the ROS suspension was deposited on a BaF_2 window and dried under room air. About 1 μL of H_2O, D_2O, or $H_2{}^{18}O$ was put beside the air-dried ROS film for humidification. The sample was sealed by another BaF_2 window with the aid of a silicon rubber O-ring, set in a cell holder made of brass, and mounted in an Oxford cryostat (DN-1704). The temperature of the sample was cooled to 80 K and controlled within 0.1 K by the cryostat equipped with an Oxford temperature controller (ITC 4) with liquid nitrogen as coolant. The cryostat has two sets of ZnSe and BaF_2 windows. Two BaF_2 windows for the sample film were also placed in the path of infrared probe light. FTIR spectra were recorded in a Bio-Rad FTS-60A/896 Spectrometer equipped with a bright IR light source (110 mW) and a highly photosensitive MCT (mercury−cadmium−tellurium) detector. The 128 interferograms at 2 cm^{-1} resolution were recorded in ~70 s and converted to the absorption spectrum by use of an interferogram that had been recorded at room temperature in the absence of the sample as the reference. Then the spectral difference before and after irradiation was calculated and compared with the base line as the difference between the two spectra without intermittent irradiation.

The light source for the irradiation was a 1 kW halogen tungsten lamp in a slide projector. The excitation light was introduced through a 5 cm water layer to remove heat and through an optical filter into the FTIR spectrometer by use of a mirror and two shutters. By examining infrared bands specific to either of rhodopsin, isorhodopsin, or bathorhodopsin, we established following irradiation conditions. (1) Irradiation with an interference filter at 501 nm (Toshiba; full width of half-maximum = 4 nm) for 5 min for the conversion of rhodopsin to bathorhodopsin or isorhodopsin to bathorhodopsin. (2) Irradiation with a red cutoff filter R-63 (Toshiba; $T_{1/2}$ = 637 nm and $T_{1/100}$ = 611 nm; >610 nm light) for 5 min for the conversion of bathorhodopsin to rhodopsin. (3) Irradiation with an orange cutoff filter O-54 (Toshiba; $T_{1/2}$ = 545 nm and $T_{1/100}$ = 528 nm; >527 nm light) for 5 min for the conversion of bathorhodopsin to isorhodopsin. It is noted that conditions 2 and 3 do not necessarily provide complete conversion from bathorhodopsin to rhodopsin and isorhodopsin, respectively (see Results).

Spectral recordings were done in the following sequences: the hydrated ROS film containing only rhodopsin was first irradiated with the 501 nm interference filter for 5 min, producing a photosteady-state mixture containing

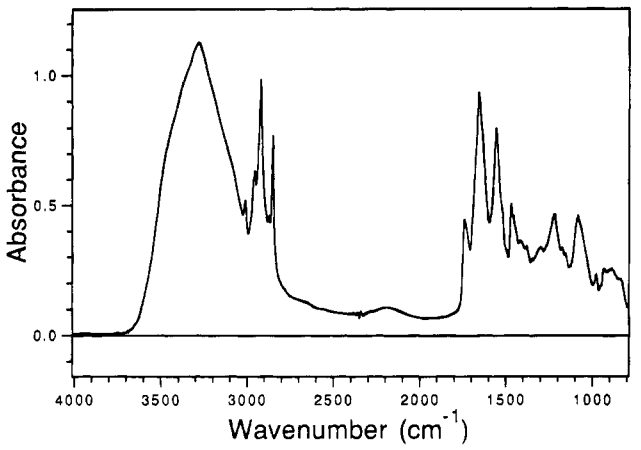

FIGURE 1: Absolute infrared absorption spectrum of the hydrated film of bovine rod outer segments (ROS) at 80 K.

predominantly bathorhodopsin. Then the sample was irradiated with either an R-63 or an O-54 filter for 5 min to convert bathorhodopsin to rhodopsin or isorhodopsin, respectively. The cycle was repeated, and 7−12 recordings were averaged. The difference spectra were finally corrected by the authentic spectra of water vapor and CO_2 gas.

RESULTS

FTIR Spectroscopy of the Hydrated Bovine ROS Film at 80 K. Figure 1 shows an absolute infrared absorption spectrum of the hydrated ROS film at 80 K. A large and broad absorption band in the 3700−3000 cm^{-1} region contains N−H and O−H stretching vibrations. The difference between two spectra measured with an interval of 5 min (Figure 2a) coincides the zero line with a deviation on the order of 10^{-4} of an absorbance unit throughout the observed window (4000−800 cm^{-1}).

Irradiation of rhodopsin with 501 nm light at 80 K for 5 min converts rhodopsin to bathorhodopsin, and subsequent irradiation with >610 nm light reverts bathorhodopsin to rhodopsin. These photoreversible reactions were repeated by recording the difference between the spectra before and after the irradiation. The bathorhodopsin minus rhodopsin (B/R) spectrum in the forward reaction (Figure 2b) and the rhodopsin minus bathorhodopsin (R/B) spectrum in the backward reaction (Figure 2c) exhibited mirror images of each other as shown by a nearly flat line for the sum of b and c (Figure 2d). Similar recordings were also conducted to obtain the bathorhodopsin minus isorhodopsin (B/I) spectrum by use of >527 nm light to convert bathorhodopsin to isorhodopsin and 501 nm light to revert isorhodopsin to bathorhodopsin (not shown).

Difference spectra in the 1800−800 cm^{-1} region in Figure 3 reproduced the previous ones (Siebert et al., 1983; Bagley et al., 1985; DeGrip et al., 1988; Ganter et al., 1989). The B/R spectrum is also identical with the previous one at 10 K (Sasaki et al., 1992). Figure 3c shows the isorhodopsin minus rhodopsin (I/R) spectrum, which was calculated from the B/R (Figure 3a) and B/I (Figure 3b) spectra by canceling the band at 921 cm^{-1} characteristic for bathorhodopsin. This spectrum is also identical with the previous one (Siebert et al., 1983; Bagley et al., 1985).

The present conditions for irradiation, however, do not result complete conversions between bathorhodopsin and rhodopsin or between bathorhodopsin and isorhodopsin. We

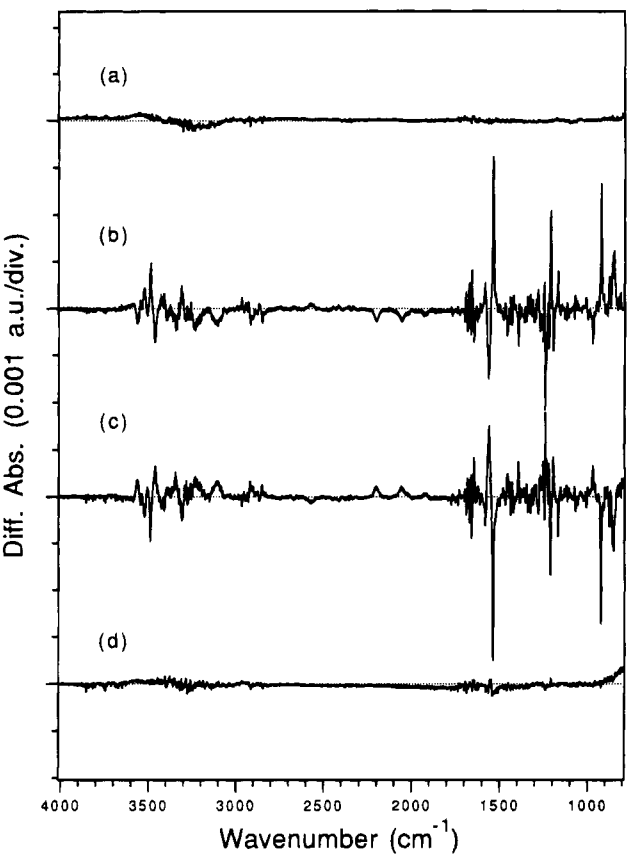

FIGURE 2: Typical data of a bovine ROS film hydrated with H_2O at 80 K. (a) The difference absorption spectrum of two spectra, each of which was scanned 128 times with an interval of 5 min. This is the base line. (b) The difference spectrum after and before irradiation with a 501 nm light for 5 min. This spectrum corresponds to that of bathorhodopsin minus rhodopsin (B/R). (c) The difference spectrum after and before irradiation with a red light (R-63) for 5 min. The spectrum corresponds to that of rhodopsin minus bathorhodopsin (R/B). (d) The sum of b and c, which is nearly flat, indicates that the two states, b and c, are photoreversible under the present irradiation conditions.

estimated the content of isorhodopsin in the B/R spectrum (Figure 3a) as 5% (B/(0.95R + 0.05I)) from the isorhodopsin-characteristic bands at 1013 and 959 cm^{-1}. Similarly, the content of rhodopsin in the B/I spectrum (Figure 3b) was estimated to be 7% (B/(0.93I + 0.07R)) from the rhodopsin-characteristic band at 1192 cm^{-1}. Nevertheless, such low extents of contamination were negligible in the analysis of the vibrational bands in the higher-frequency side.

The difference spectra in the 1800−800 cm^{-1} region contain changes not only in the chromophore but also in the protein. Figure 4 shows a closer look of the same spectra for the carboxylic C=O stretching mode in the 1790−1710 cm^{-1} region. Two positive peaks at 1773 and 1735 cm^{-1} and three negative peaks at 1767, 1740, and 1727 cm^{-1} were observed in the 1790−1710 cm^{-1} region of the B/R spectrum (Figure 4a). In addition to the common peaks, the B/I spectrum displayed an additional positive peak at 1722 cm^{-1} (Figure 4b). These facts indicate that the 1722 cm^{-1} peak is present in both rhodopsin and bathorhodopsin but absent only in isorhodopsin. By referring the assignments in the spectrum of metarhodopsin-II vs rhodopsin of mutants (Fahmy et al., 1993), the rhodopsin-specific bands are identified: the carboxyl C=O stretch of Asp83 at 1767 cm^{-1}, the carboxyl C=O stretch of Glu122 at 1734 cm^{-1}, and the peptide carbonyl C=O stretch of Glu122 at 1727 cm^{-1}. The

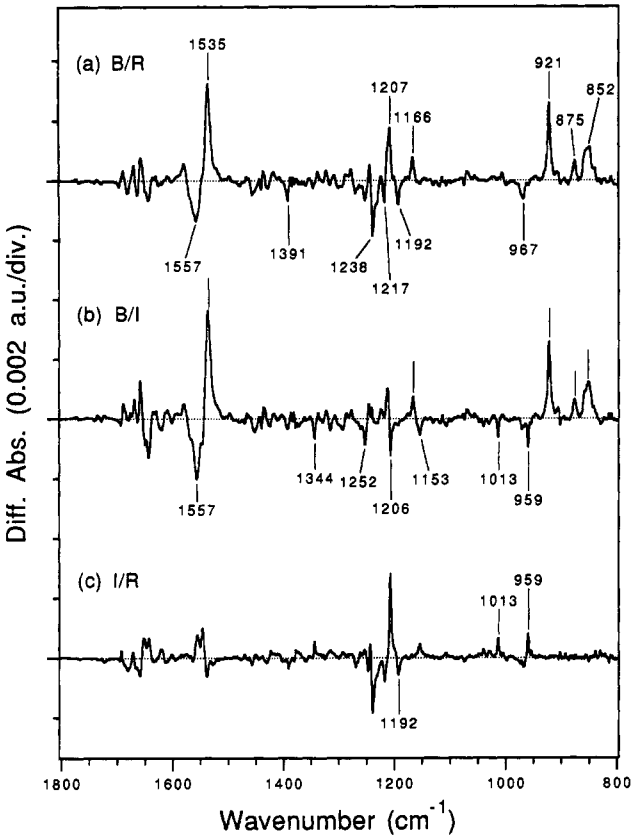

FIGURE 3: B/R (a), B/I (b), and I/R (c) spectra in the 1800−800 cm^{-1} region. The B/R and B/I spectra are the average of 7 and 10 spectra such as shown in Figure 2, respectively, and normalized so as to possess the same positive intensity at 921 cm^{-1}. The I/R spectrum (c) is obtained by subtracting the B/I spectrum (b) from the B/R spectrum (a).

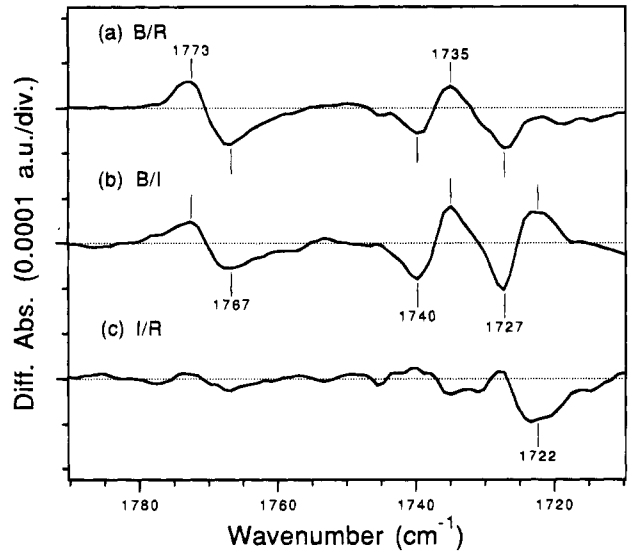

FIGURE 4: B/R (a), B/I (b), and I/R (c) spectra in the 1790−1710 cm^{-1} region. Each spectrum was taken from Figure 3.

negative peak at 1740 cm^{-1} in Figure 4a,b is probably due to the 1734 cm^{-1} band of Glu122. The 1722 cm^{-1} band, which is absent in isorhodopsin, cannot be identified.

Difference Spectra of Rhodopsin, Bathorhodopsin, and Isorhodopsin in the 3700−3430 cm^{-1} Region. Figure 5 shows the B/R (a), B/I (b), and I/R (c) spectra in the 3700−3430 cm^{-1} region. The present FTIR measurements are highly sensitive to detect such a small positive peak at 3653

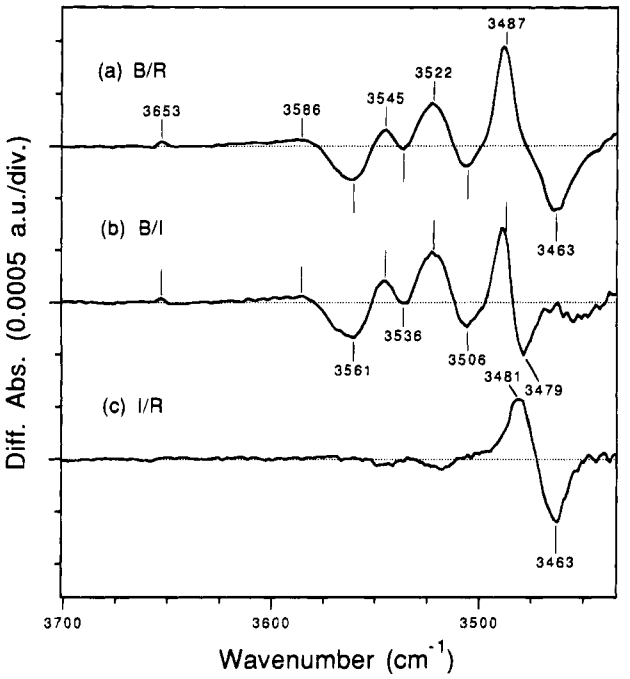

FIGURE 5: B/R (a), B/I (b), and I/R (c) spectra in the 3700−3430 cm^{-1} region. Each spectrum was taken from Figure 3.

cm^{-1} in the B/R spectrum (Figure 5a) with 0.000 04 (4×10^{-5}) of an absorbance unit. The B/R spectrum further displays positive peaks at 3586, 3545, 3522, and 3487 cm^{-1} and negative peaks at 3561, 3506, and 3463 cm^{-1}. The spectral features of both the B/R and B/I spectra are identical with each other except for a negative band at 3479 cm^{-1} in the B/I spectrum (Figure 5b) instead of the 3463 cm^{-1} band in the B/R spectrum (Figure 5a). In the I/R spectrum (Figure 5c), this difference is clearly seen as a bilobe with a positive band at 3481 cm^{-1} and a negative band at 3463 cm^{-1}. The frequency of the band in isorhodopsin is more likely to be 3481 cm^{-1} than 3479 cm^{-1} because the frequencies in bathorhodopsin and isorhodopsin are close to each other in Figure 5b, providing an apparent lower-frequency shift in isorhodopsin. Thus, the 3463 cm^{-1} band of rhodopsin shifts to 3481 cm^{-1} in isorhodopsin and to 3487 cm^{-1} in bathorhodopsin. No other differences are detected in the I/R spectrum (Figure 5c).

Identification of the Bands in the 3700−3430 cm^{-1} Region. The O−H and N−H stretching vibrations which form weak H-bonding are expected to be observed in the 3700−3430 cm^{-1} region. Upon hydration with D_2O, the hydrogen atoms of O−H and N−H bonds would exchange for deuterium, so that the O−D or N−D stretching vibrations shift by ~1000 cm^{-1}, unless the environment makes these bonds inaccessible to the deuteration. The O−H band of water can be identified by hydrating the ROS film with $H_2{}^{18}O$ to yield the band downshifted by ~10 cm^{-1}.

In Figure 6, the B/R (a) and B/I (b) spectra in D_2O (solid lines) were compared with the corresponding spectra in H_2O (dotted lines). Although all the bands above 3500 cm^{-1} looked to shift in D_2O, some bands insensitive to D_2O remained in the D_2O spectra. Thus, the difference spectrum for the D_2O-sensitive bands were obtained by the subtraction of the spectrum in D_2O (H_2O − D_2O spectra in Figure 6a,b). In this way, a negative band was revealed at 3536 cm^{-1} in both the B/R and B/I spectra. The D_2O-sensitive bands are present at 3653, 3586, 3547, 3525, and 3467 cm^{-1} for

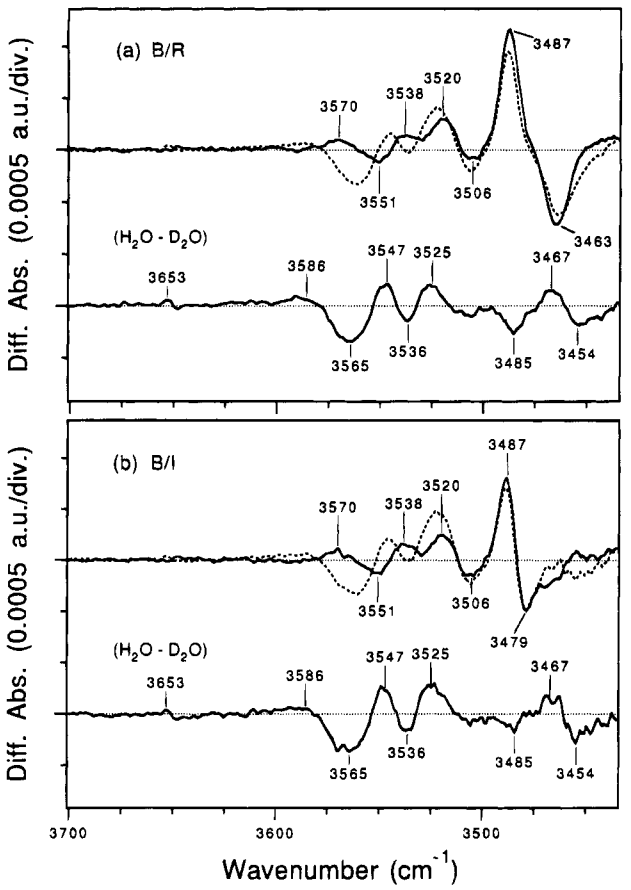

FIGURE 6: Effect of deuterium substitution in the 3700−3430 cm^{-1} region for the B/R (a) and B/I (b) spectra. Solid and dotted lines in the upper side represent the difference spectra upon photoreaction for the samples hydrated with D_2O and H_2O, respectively. The spectrum in the lower side is the difference of the two spectra (H_2O − D_2O).

bathorhodopsin and at 3565, 3536, 3485, and 3454 cm^{-1} for rhodopsin and isorhodopsin. The bands of rhodopsin, bathorhodopsin, and isorhodopsin at 3463, 3487, and 3479 cm^{-1} (3481 cm^{-1} in Figure 5c), respectively, are insensitive to D_2O and remain in the D_2O spectra (solid lines). The apparent increase in intensity of these bands upon hydration with D_2O is due to the presence of the D_2O-sensitive bands at 3485 cm^{-1} (−) and 3467 cm^{-1} (+) as revealed in the H_2O − D_2O spectra. Those bands in the H_2O − D_2O spectra could be due to the O−H stretching vibration of water. However, the direct proof is provided by the spectral shift upon substitution with $H_2{}^{18}O$.

Figure 7 shows the spectra of the samples hydrated with H_2O (dotted lines) and $H_2{}^{18}O$ (solid lines). Both the B/R and the B/I spectra in $H_2{}^{18}O$ showed a positive peak at 3517 cm^{-1} and a negative peak at 3555 cm^{-1}, which shifted from the 3522 and 3561 cm^{-1} peaks in H_2O, respectively. The peaks at 3545 and 3536 cm^{-1} were also shifted in $H_2{}^{18}O$. Thus, though they contain D_2O-insensitive bands in those peaks in H_2O, all of the D_2O-sensitive bands in the 3580−3510 cm^{-1} region in the H_2O − D_2O spectra in Figure 6 should be due to water O−H stretching vibrations. The negative band at 3565 cm^{-1} has an amplitude almost twice as intense as the other bands. Generally, stronger H-bonding of the O−H lowers the O−H stretching frequency and increases its amplitude (Glew & Rath, 1971). These facts suggest that the 3565 cm^{-1} band with weaker H-bonding is

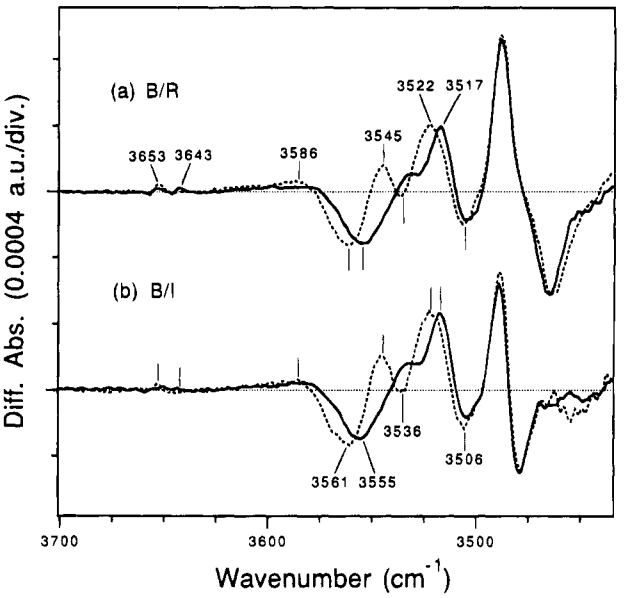

FIGURE 7: Identification of the O−H stretching mode of water molecule in the B/R (a) and B/I (b) spectra. Solid and dotted lines represent the difference spectra hydrated with $H_2{}^{18}O$ and H_2O, respectively.

composed of two or more O−H stretching vibration bands.

On the other hand, the negative peak at 3506 cm^{-1} seems not to shift in $H_2{}^{18}O$ (Figure 7). The D_2O-sensitive small positive band at 3586 cm^{-1} (H_2O − D_2O spectra in Figure 6) is difficult to be identified as water O−H, although this peak looks shifted in $H_2{}^{18}O$ (Figure 7). The apparent shift of this small and broad peak may be a result of the downshift of the negative peak at 3561 cm^{-1}. Half of the area under the small positive peak at 3653 cm^{-1} shifted to 3643 cm^{-1} while the other half remained unshifted. This indicates that two O−H stretches contribute the 3653 cm^{-1} peak, and at least one O−H is due to water. It is noted that the integrated amplitude under the positive peak at 3653 cm^{-1} is about one-thirtieth of that under the negative peak at 3561 cm^{-1}.

Difference Spectra in the 2750−2470 cm^{-1} Region. Figure 8 shows the B/R and B/I spectra in the 2750−2470 cm^{-1} region. When hydrated with H_2O (Figure 8a,b), the positive bands are observed at 2574 and 2556 cm^{-1}. The frequencies of these bands can be accounted for by S−H stretch of some cysteine residues, although combination of bands at lower frequencies cannot be excluded. Indeed, as revealed by Rath et al. (1994) on metarhodopsin-II, a corresponding band was observed at 1838 cm^{-1} in D_2O (data not shown). Thus, we find a spectral change for the S−H stretch of cysteine residues upon conversion from rhodopsin (isorhodopsin) to bathorhodopsin. It is noted that the negative band corresponding to the S−H mode of rhodopsin is absent, as the difference spectrum between metarhodopsin-II and rhodopsin (Rath et al., 1994). In addition, the absorbance change was slightly smaller in the B/I spectrum (Figure 8b) than in the B/R spectrum (Figure 8a).

The difference FTIR spectrum of the ROS film hydrated with D_2O shows the O−D and N−D stretching vibrations in this frequency region (2750−2470 cm^{-1}). Both B/R (Figure 8c) and B/I (Figure 8d) spectra show three positive bands at 2607, 2567, and 2525 cm^{-1}. Among them, the 2607 cm^{-1} band probably corresponds to the 3547 cm^{-1} band in Figure 6. The factor for the shift, 1.36, is in good agreement

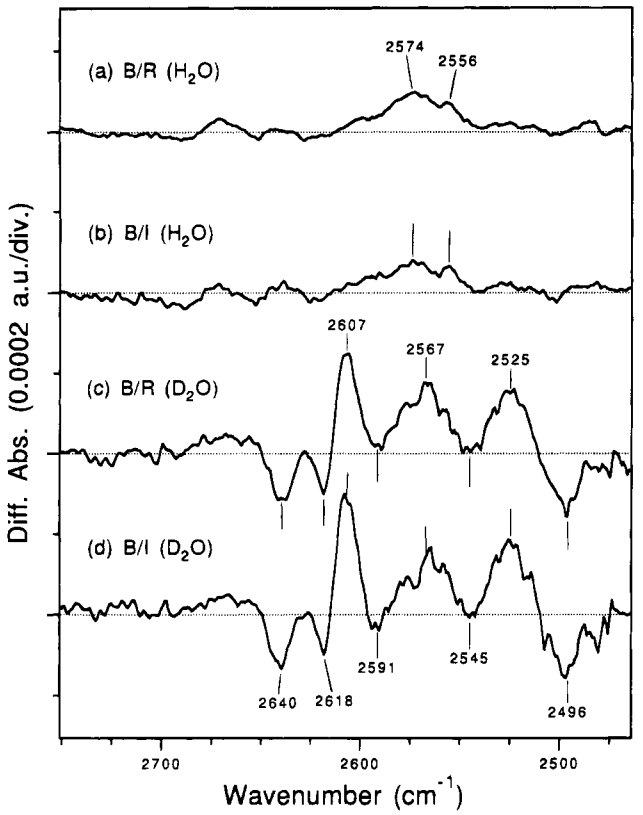

FIGURE 8: B/R (a) and B/I (b) spectra hydrated with H_2O and the B/R (c) and B/I (d) spectra hydrated with D_2O in the 2750−2470 cm^{-1} region. Each spectrum was taken from Figure 6.

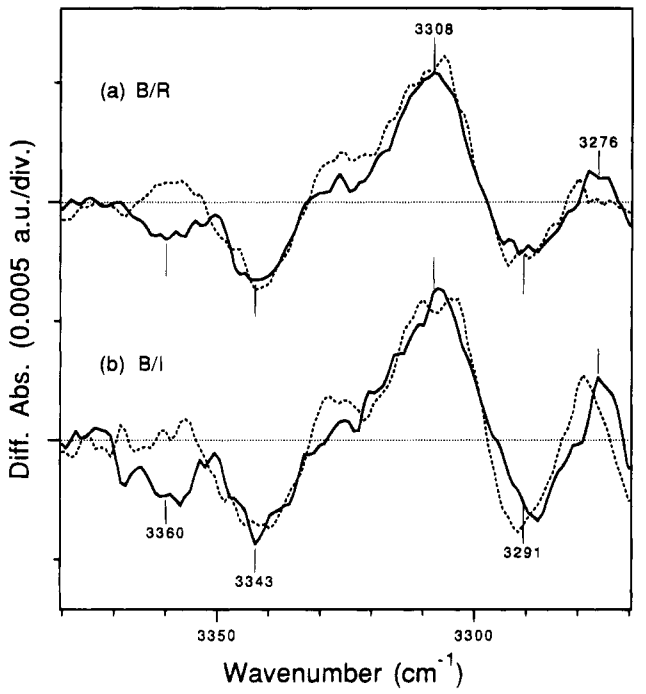

FIGURE 9: B/R (a) and B/I (b) spectra in the 3380−3270 cm^{-1} region. Solid and dotted lines represent the difference spectra hydrated with H_2O and D_2O, respectively. Each spectrum was taken from Figure 6.

with that calculated from the reduced mass between O−H and O−D (1.37). Since the downshift of the O−H stretching mode for each band depends on the environment, the spectral feature in this region is not necessarily the same as that in the higher-frequency region (H_2O − D_2O spectra in Figure 6). In the negative side, the spectra possess three distinct (2640, 2618, and 2496 cm^{-1}) and two possible (2591 and 2545 cm^{-1}) bands. It seems that the negative band at 3565 cm^{-1} with an amplitude about twice the other water O−H bands (Figure 6) split into two at 2640 and 2618 cm^{-1} in D_2O (Figure 8). The present FTIR spectroscopy thus implies that at least three water O−H stretching modes change their frequencies in the conversion of rhodopsin to bathorhodopsin.

Difference Spectra in the 3380−3270 cm^{-1} Region. The amide-A of the peptide N−H (N−H stretching mode) has been reported to appear near 3320−3270 cm^{-1} (Krimm & Bandekar, 1986; Lin-Vien et al., 1991). This is also the case for rhodopsin (Rothschild et al., 1980). Thus, the analysis of the 3380−3270 cm^{-1} region will lead to an understanding of the structural change of the peptide backbone in rhodopsin. The assignment of the N−H stretching mode of the protonated Schiff base, which is expected to appear in this region, is also of importance for the structural change around the Schiff base.

Figure 9 shows the B/R (a) and B/I (b) spectra in the 3380−3270 cm^{-1} region in both H_2O (solid lines) and D_2O (dotted lines). In spite of the disturbance due to large absorption of water (Figure 1), the spectra were obtained reproducibly. Both of the difference spectra displayed two positive bands at 3308 and 3276 cm^{-1} and three negative bands at 3360, 3343, and 3291 cm^{-1}. Three peaks (3308, 3291, and 3276 cm^{-1}) are located in the amide-A region (3320−3270 cm^{-1}). The negative 3343 cm^{-1} band could be also regarded as an amide-A. If so, the two rhodopsin (isorhodopsin) bands at 3343 and 3291 cm^{-1} experience a downshift on conversion to bathorhodopsin to 3308 and 3276 cm^{-1}, respectively. These bands were insensitive to D_2O (dotted lines), indicating that these N−H bonds are buried in the protein. Since the spectral downshift represents stronger H-bonding formation, formation of bathorhodopsin is accompanied by the increase of H-bonding of the amide N−H.

The negative 3360 cm^{-1} band, which was sensitive to D_2O substitution, appeared in the both B/R and B/I difference spectra, though the corresponding positive band of bathorhodopsin was not clearly seen in this region. This band is a candidate of the N−H stretching mode of the Schiff base.

DISCUSSION

The present FTIR spectroscopy provided difference spectra among rhodopsin, bathorhodopsin, and isorhodopsin at 80 K in the whole mid-infrared region (4000−800 cm^{-1}). The spectral change in the >1800 cm^{-1} region was accurately measured for the first time. If we neglect the contribution of overtones or combination bands of the lower-frequency modes and regard the Schiff base as part of the protein, the chromophore has only C−H stretching vibrations in the 3100−2800 cm^{-1} region. All other chromophore modes are located below 1800 cm^{-1} except for the N−H stretch of the Schiff base in the higher-frequency region. Thus, the spectral change in the high-frequency region (3700−3430 cm^{-1}, 3380−3270 cm^{-1}, and 2750−2470 cm^{-1} in the present study) is a good probe to resolve changes in the protein structure and internal water molecules. There are other notable spectral changes in the negative absorption bands at 2200 and 2000 cm^{-1} in the B/R spectrum (Figure 2b). The analysis of these bands is now in progress.

Water Structural Change upon Photoisomerization. The present FTIR spectroscopy revealed three water O−H (two bands at 3565 cm^{-1} and one at 3536 cm^{-1})[2] downshifted upon photoisomerization, indicating stronger H-bonding formation. It should be noted that the spectral feature in the water O−H region is identical in the B/R and B/I spectra (Figure 5). This indicates that the water molecules, which change their structure upon formation of bathorhodopsin, remain in the same structure in rhodopsin and isorhodopsin and make stronger H-bonding states upon formation of bathorhodopsin. Among water molecules in the two water binding sites in bacteriorhodopsin (Yamazaki et al., 1995b), only the water molecules around the Schiff base undergo structural changes in the K intermediate, an analogous state to bathorhodopsin (Fischer et al., 1994; H. Kandori and A. Maeda, unpublished observation). In rhodopsin, water molecules around the Schiff base are also expected to change their structures upon formation of bathorhodopsin.

Previous studies on the later intermediates of rhodopsin (Maeda et al., 1993) showed that the water O−H stretching vibration appears at 3533 cm^{-1} for lumirhodopsin and metarhodopsin-I and 3641 cm^{-1} for metarhodopsin-II. The broad feature in the 3610−3540 cm^{-1} region for rhodopsin might also be due to water O−H stretch, though it is not well characterized. The water O−H stretch at 3565 cm^{-1} for rhodopsin in the present study (Figure 6) would correspond to one of the bands in the broad feature for rhodopsin. In the case of bacteriorhodopsin, the water bound to the Schiff base displays its O−H stretch at 3642 cm^{-1} (Maeda et al., 1994). On the other hand, the presence of the water O−H stretches of rhodopsin in the 3580−3510 cm^{-1} region (Figures 6 and 7) suggests that an H-bonding network around the Schiff base is stronger than bacteriorhodopsin.

There were D_2O-insensitive bands in the 3700−3500 cm^{-1} region. These bands could be due to the O−H stretching mode of (i) a water molecule, (ii) Ser, Thr, or Tyr, or (iii) a protonated Asp or Glu. It is considered that the environments of the β-ionone ring and the polyene chain of the chromophore are highly hydrophobic and inaccessible to external water. Therefore, the O−H in this moiety, which may be inexchangeable to D_2O, would change in structure upon formation of bathorhodopsin.

It should be noted that, in addition to the water O−H in the 3600−3500 cm^{-1} region, another water band was observed at 3653 cm^{-1} (Figure 5). The frequency corresponds to the free O−H stretching mode without H-bonding. This water is unlikely to interact with the Schiff base because the amplitude is much smaller to regard it as a single water molecule. The water possessing this free O−H may be present in another part of the protein and changes the environment slightly upon isomerization.

Spectral Change of the S−H Stretching Vibration. Rath et al. (1994) observed the absorbance increase of the 2550 and 2530 cm^{-1} bands due to the cysteine S−H stretching modes upon formation of metarhodopsin-II. The bands were not observed in the metarhodopsin-I/rhodopsin difference spectrum. Interestingly, we observed a similar absorbance increase upon formation of bathorhodopsin at slightly higher frequency, 2574 and 2556 cm^{-1} (Figure 8). The frequency of the S−H stretching changes only in a narrow region of 2580−2525 cm^{-1}, and the molar extinction coefficient increases markedly upon H-bonding formation (Spurr & Byers, 1958; Alben et al., 1974). Thus, the present observation can be accounted for by the increase of H-bonding strength. The absorbance increase is slightly larger in the B/R spectrum than the B/I spectrum (Figure 8), suggesting that H-bonding of the S−H group is stronger in isorhodopsin than rhodopsin.

The two cysteine residues deeply embedded in the membrane (Cys167 and Cys264; Figure 10) could be candidates that are perturbed in the vicinity of the chromophore. On the other hand, Cys222, which is reactive to a spin-labeling compound at the membrane surface of rhodopsin (Farahbakhsh et al., 1992), may not be involved. Thus, the analysis in the S−H stretch region suggested an increase in the H-bonding of at least two cysteine residues, Cys167 and Cys264, upon formation of bathorhodopsin, which will be directly evidenced by use of mutants.

Peptide N−H Stretching Vibration. The spectral change shown in Figure 9 is most likely to have originated from the N−H stretching mode of the peptide backbone, which was reported to appear in the 3320−3270 cm^{-1} region (Rothschild et al., 1980; Krimm & Bandekar, 1986; Lin-Vien et al., 1991). The negative rhodopsin-specific bands at 3343 and 3291 cm^{-1} seem to shift to 3308 and 3276 cm^{-1}, respectively, upon formation of bathorhodopsin. The negative bands were similar in isorhodopsin. These results indicate that H-bonding of the peptide N−H becomes stronger upon photoisomerization.

In addition to the peptide N−H stretches, the N−H stretch of the protonated Schiff base could appear in the 3320−3270 cm^{-1} region (Figure 9). While the Schiff base environment in rhodopsin has been argued through its C=N stretching mode (Deng & Callender, 1987; Palings et al., 1987; Maeda, 1995), identification of the Schiff base N−H stretching frequency is also important. The present observation of the D_2O-sensitive 3360 cm^{-1} band provided one of the candidates as the Schiff base N−H stretching mode (Figure 9).

Mechanism of the Storage of the Acquired Light Energy in Bathorhodopsin: Probing from the Protein Side. The efficient photoisomerization in rhodopsin leads to formation of bathorhodopsin through a primary intermediate, photorhodopsin (Shichida et al., 1984). It is well-known that bathorhodopsin is in a higher energy state than rhodopsin by ~35 kcal/mol (Cooper, 1979). This indicates that ~65% of the acquired light energy is stored in bathorhodopsin. Resonance Raman spectroscopy of bathorhodopsin revealed the highly constrained structure of the all-trans chromophore by probing mainly the HOOP modes (Eyring et al., 1982; Palings et al., 1989).

The present FTIR spectroscopy showed some energy storage in the O−H, S−H, and N−H vibrational modes of the protein and the internal water molecules. We revealed that H-bondings of three (or more) water O−H, two cysteine S−H, and at least two peptide N−H become stronger in bathorhodopsin. The results show that a part of the energy first absorbed in the chromophore is transferred to these

[2] This is not necessarily indicative of three water molecules because there are two O−H in a water. However, each O−H stretch mode is likely to originate from a different water molecule, since the O−H stretch in the >3500 cm^{-1} region represents weak H-bonding and two weak O−H bonds in a single bound water are unlikely (Kandori et al., 1995).

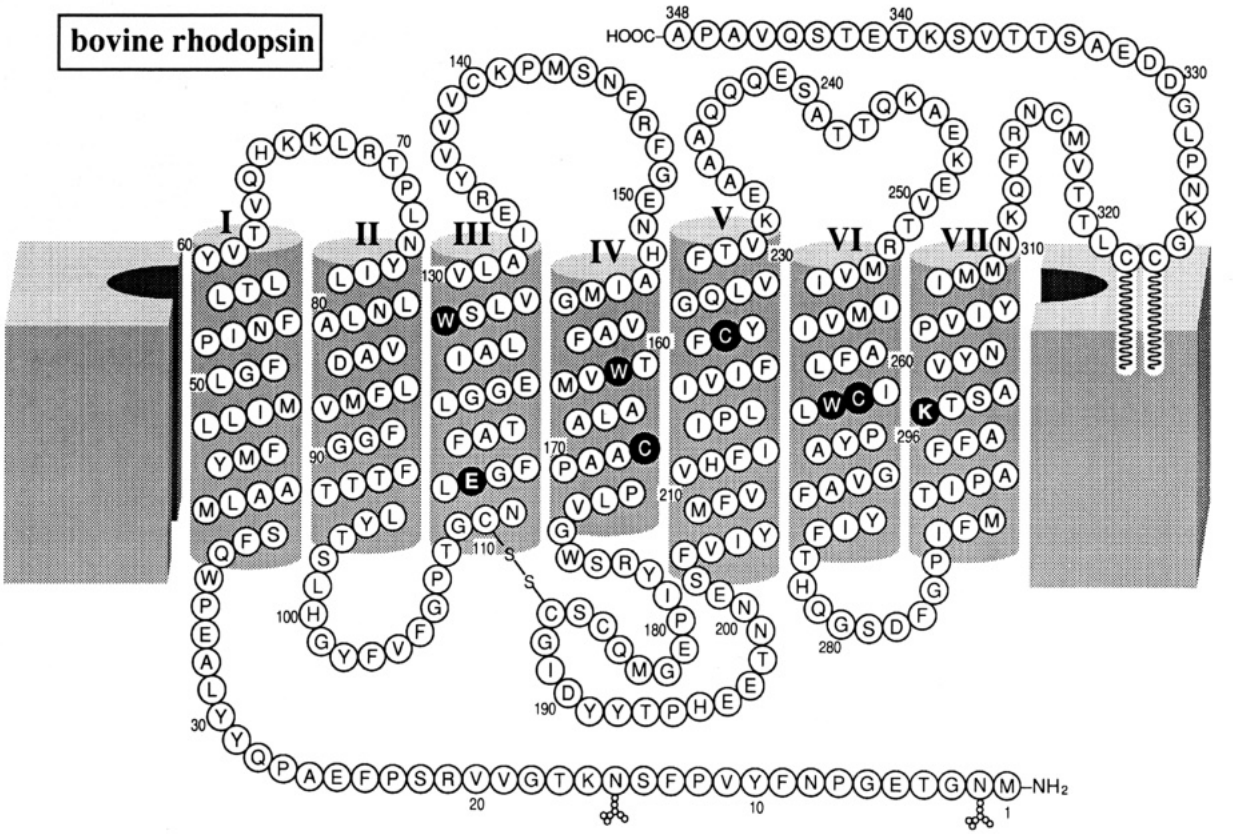

FIGURE 10: Two-dimensional model of bovine rhodopsin. The following residues are highlighted; Lys296 forming a Schiff base with 11-cis retinal, Glu113 as the protonated Schiff base counterion, and membrane-embedded tryptophan and cysteine residues.

protein parts already in bathorhodopsin. According to the schematic model of the chromophore structure in Figure 11, the longer axis of the all-trans chromophore of bathorhodopsin would be accommodated only by forming a twisted chromophore. Stronger H-bondings of the protein part may be enforced by such a twisted chromophore in bathorhodopsin.

Deuterium-Insensitive N−H Stretching Mode of Rhodopsin at 3463 cm^{-1} That Specifically Interacts with the Chromophore. The B/R and B/I spectra showed a remarkably similar feature in the high-frequency region (Figures 5, 8, and 9). This indicates the structural similarity of the protein moiety in rhodopsin and isorhodopsin. One notable difference between rhodopsin and isorhodopsin can be seen in the 3490−3460 cm^{-1} region of the spectra (Figure 5). The band at 3463 cm^{-1} in rhodopsin shifts to 3487 cm^{-1} in bathorhodopsin and to 3481 cm^{-1} in isorhodopsin. These bands may have a different origin from the negative 3473 cm^{-1} band in the lumirhodopsin/rhodopsin and metarhodopsin-I/rhodopsin spectra (Maeda et al., 1993).

The free O−H stretch has been reported at 3640−3610 cm^{-1} for alcohols and at >3600 cm^{-1} for water. The sharp peak of this band (half-width: ~10 cm^{-1}) could not be due to the O−H stretch, which would appear as a broad band in this region due to the formation of H-bonding. On the other hand, those frequencies are located nearly at the upper limit of N−H stretches, indicating that they originate from the free N−H stretching mode. Thus, the origin of the band at 3463 cm^{-1} in rhodopsin is likely to be a free N−H inexchangeable to D_2O, though we cannot exclude the possibility that the corresponding bands in bathorhodopsin (3487 cm^{-1}) and isorhodopsin (3481 cm^{-1}) are ascribable to different N−H.

The fact that the band is insensitive to D_2O suggests that the N−H is located in the hydrophobic environment near the chromophore. The frequency shift may be explained in terms of an induced dipole between the N−H and the retinal skeleton. In this case, when the distance between the N−H and the chromophore is closer, the electrostatic interaction forming the induced dipole becomes stronger, resulting in the lower-frequency shift of the N−H stretch. On the basis of this argument, the higher-frequency shifts by 24 and 18 cm^{-1} for bathorhodopsin and isorhodopsin, respectively, may have originated from a lengthening of the distance between the N−H and the retinal skeleton.

As schematically illustrated in Figure 11, the rhodopsin chromophore is fixed at both ends with the β-ionone ring through hydrophobic interaction (Matsumoto & Yoshizawa, 1975) and through the α-carbon of Lys296 to the peptide backbone (dense circles). The present FTIR results revealed that the protein structure probed through O−H, S−H, and peptide N−H stretching modes was almost identical between rhodopsin and isorhodopsin. More efficient isomerization in rhodopsin than isorhodopsin might be thus explained in terms of different geometrical relation of a fixed N−H (open circles in Figure 11) with the retinal skeleton in two isomers. Specific interaction between the N−H and the chromophore in the electronic ground state might play an important role to isomerize the chromophore in the excited state.

A similar sharp and strong absorption band in the L intermediate of bacteriorhodopsin at 3486 cm^{-1} (Maeda et al., 1992a) was assigned to the indole N−H stretch of Trp182 by a shift in [^{15}N]indole-labeled bacteriorhodopsin (Maeda et al., 1992b) and by use of mutants (Yamazaki et al., 1995a). This mode is also insensitive to D_2O. The indole N−H of Trp182 showed a large infrared intensity by interacting with

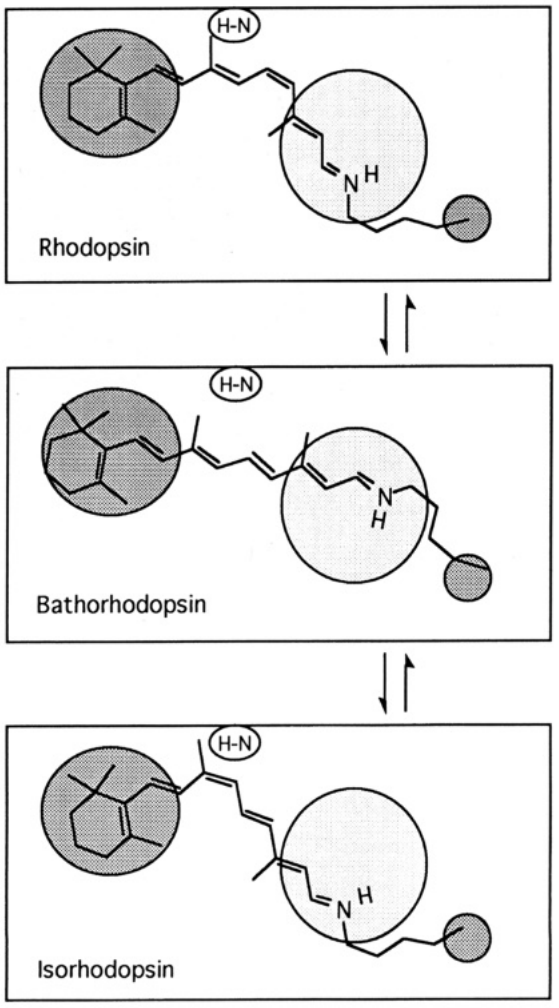

FIGURE 11: Schematic drawing of the structure of the chromophore in rhodopsin, bathorhodopsin and isorhodopsin. Two dense circles at the β-ionone ring and the α-carbon of Lys296 indicate the strong binding of the chromophore to the protein through hydrophobic interaction and covalent binding, respectively. The flexible Schiff base moiety that is in the hydrophilic environment is covered by less dense circles, where at least three water molecules are contained. The deuterium-insensitive N−H (open circles), which is most likely to be a tryptophan indole, interacts with the retinal skeleton in a different manner among three isomeric states. In this scheme, the interaction is done through the 9-methyl group of the chromophore. Light leads to the reversible reaction among the 11-cis (rhodopsin), all-trans (bathorhodopsin), and 9-cis (isorhodopsin) forms.

the chromophore through the 9-methyl group in the L intermediate. This interaction plays an important role in the primary intramolecular proton transfer from the Schiff base to the proton acceptor, Asp85, in the L-to-M conversion process.

The N−H stretches in the present results on rhodopsin may be explained in analogy with these results on bacteriorhodopsin. Among Trp126, Trp161, and Trp265 embedded in the membrane and highly conserved through vertebrate photoreceptors (Figure 10), Trp161 shows no specific interaction with the chromophore (Nakayama & Khorana, 1991). Trp265 is located at the same position in the middle of the sixth helix in rhodopsin as Trp182 in bacteriorhodopsin. The photoaffinity studies, however, revealed that Trp265 is located close to the β-ionone ring (Nakayama & Khorana, 1990; Zhang et al., 1994), not near the 9-methyl group. Pigment formation of Trp126 mutants significantly reduced with 11-cis retinal fixed by the six-membered ring (Ridge et al., 1992), implying that Trp126 is a residue that interacts with the central part of the chromophore. Direct proof will be obtained by the FTIR study of mutants in the future.

REFERENCES

Alben, J. O., Bare, G. H., & Bromberg, P. A. (1974) *Nature 252*, 736−738.

Bagley, K. A., Balogh-Nair, V., Croteau, A. A., Dollinger, G., Ebrey, T. G., Eisenstein, L., Hong, M. K., Nakanishi, K., & Vittitow, J. (1985) *Biochemistry 24*, 6055−6071.

Becker, R. S., & Freedman, K. (1985) *J. Am. Chem. Soc. 107*, 1477−1485.

Birge, R. R. (1990) *Biochim. Biophys. Acta 1016*, 293−327.

Cooper, A. (1979) *Nature 282*, 531−533.

Dartnall, H. J. A. (1967) *Vision Res. 8*, 339−358.

DeGrip, W. J., Gray, D., Gillespie, J., Bovee, P. H. M., van den Berg, E. M. M., Lugtenburg, J., & Rothschild, K. J. (1988) *Photochem. Photobiol. 48*, 497−504.

Deng, H., & Callender, R. H. (1987) *Biochemistry 26*, 7418−7426.

Emeis, D., Kühn, H., Reichert, J., & Hofmann, K. P. (1982) *FEBS Lett. 143*, 29−34.

Eyring, G., Curry, B., Broek, A., Lugtenburg, J., & Mathies, R. A. (1982) *Biochemistry 21*, 384−393.

Fahmy, K., Jäger, F., Beck, M., Zvyaga, T. A., Sakmar, T. P., & Siebert, F. (1993) *Proc. Natl. Acad. Sci. U.S.A. 90*, 10206−10210.

Fahmy, K., Siebert, F., & Sakmar, T. P. (1994) *Biochemistry 33*, 13700−13705.

Farahbakhsh, Z. T., Altenbach, C., & Hubbell, W. L. (1992) *Photochem. Photobiol. 56*, 1019−1033.

Fischer, W. B., Sonar, S., Marti, T., Khorana, H. G., & Rothschild, K. J. (1994) *Biochemistry 33*, 12757−12762.

Franke, R. R., König, B., Sakmar, T. P., Khorana, H. G., & Hofmann, K. P. (1990) *Science 250*, 123−125.

Ganter, U. M., Schmid, E. D., Perez-Sala, D., Rando, R. R., & Siebert, F. (1989) *Biochemistry 28*, 5954−5962.

Glew, D. N., & Rath, N. S. (1971) *Can. J. Chem. 49*, 837−856.

Jäger, F., Farmy, K., Sakmar, T. P., & Siebert, F. (1994) *Biochemistry 33*, 10878−10882.

Kakitani, T., Matsuda, N., Hatano, Y., Shichida, Y., & Kakitani, H. (1992) *Photochem. Photobiol. 56*, 989−993.

Kandori, H., Matuoka, S., Nagai, H., Shichida, Y., & Yoshizawa, T. (1988) *Photochem. Photobiol. 48*, 93−97.

Kandori, H., Matuoka, S., Shichida, Y., & Yoshizawa, T. (1989a) *Photochem. Photobiol. 49*, 181−184.

Kandori, H., Shichida, Y., & Yoshizawa, T. (1989b) *Biophys. J. 56*, 453−457.

Kandori, H., Yamazaki, Y., Sasaki, J., Needleman, R., Lanyi, J. K., & Maeda, A. (1995) *J. Am. Chem. Soc. 117*, 2118−2119.

König, B., Arendt, A., McDowell, J. H., Kahlert, M., Hargrave, P. A., & Hofmann, K. P. (1989) *Proc. Natl. Acad. Sci. U.S.A. 86*, 6878−6882.

Koyama, Y., Kubo, K., Komori, M., Yasuda, H., & Mukai, Y. (1991) *Photochem. Photobiol. 54*, 433−443.

Krimm, S., & Bandekar, J. (1986) *Adv. Protein Chem. 38*, 183−364.

Kropf, A., & Hubbard, R. (1958) *Ann. N. Y. Acad. Sci. 74*, 266−280.

Lin, S. W., Sakmar, T. P., Franke, R. R., Khorana, H. G., & Mathies, R. A. (1992) *Biochemistry 31*, 5105−5111.

Lin-Vien, D., Colthup, N. B., Fateley, W. G., & Grasselli, J. G. (1991) *The Handbook of Characteristic Frequencies of Organic Molecules*, Academic Press, San Diego.

Liu, R. S. H., & Asato, A. E. (1985) *Proc. Natl. Acad. Sci. U.S.A. 82*, 259−263.

Maeda, A. (1995) *Israel J. Chem.* (in press).

Maeda, A., Sasaki, J., Shichida, Y., & Yoshizawa, T. (1992a) *Biochemistry 31*, 462−467.

Maeda, A., Sasaki, J., Ohkita, Y. J., Simpson, M., & Herzfeld, J. (1992b) *Biochemistry 31*, 12543−12545.

Maeda, A., Ohkita, Y. J., Sasaki, J., Shichida, Y., & Yoshizawa, T. (1993) *Biochemistry 32*, 12033−12038.

Maeda, A., Sasaki, J., Yamazaki, Y., Needleman, R., & Lanyi, J. K. (1994) *Biochemistry 33*, 1713−1717.

Matsumoto, H., & Yoshizawa, T. (1975) *Nature 258*, 523−526.
Nakayama, T. A., & Khorana, H. G. (1990) *J. Biol. Chem. 265*, 15762−15769.
Nakayama, T. A., & Khorana, H. G. (1991) *J. Biol. Chem. 266*, 4269−4275.
Nathans, J. (1990) *Biochemistry 29*, 9746−9752.
Nathans, J. (1992) *Biochemistry 31*, 4923−4931.
Palings, I., Pardoen, J. A., van den Berg, E., Winkel, C., Lugtenburg, J., & Mathies, R. A. (1987) *Biochemistry 26*, 2544−2556.
Palings, I., van den Berg, E. M. M., Lugtenburg, J., & Mathies, R. A. (1989) *Biochemistry 28*, 1498−1507.
Rath, P., DeCaluwe, L. L. J., Bovee-Geurts, P. H. M., DeGrip, W. J., & Rothschild, K. J. (1993) *Biochemistry 32*, 10277−10282.
Rath, P., Bovee-Geurts, P. H. M., DeGrip, W. J., & Rothschild, K. J. (1994) *Biophys. J. 66*, 2085−2091.
Ridge, K. D., Bhattacharya, S., Nakayama, T. A., & Khorana, H. G. (1992) *J. Biol. Chem. 267*, 6770−6775.
Rothschild, K. J., Sanches, R., & Hsiao, T. L. (1980) *Biophys. J. 31*, 53−64.
Sakmar, T. P., Franke, R. R., & Khorana, H. G. (1989) *Proc. Natl. Acad. Sci. U.S.A. 86*, 8309−8313.
Sasaki, J., Maeda, A., Shichida, Y., Groesbeek, M., Lugtenburg, J., & Yoshizawa, T. (1992) *Photochem. Photobiol. 56*, 1063−1071.
Schertler, G. F. X., Villa, C., & Henderson, R. (1993) *Nature 362*, 770−772.
Schoenlein, R. W., Peteanu, L. A., Mathies, R. A., & Shank, C. V. (1991) *Science 254*, 412−415.
Shichida, Y. (1986) *Photobiochem. Photobiophys. 13*, 287−307.
Shichida, Y., Matuoka, S., & Yoshizawa, T. (1984) *Photobiochem. Photobiophys. 7*, 221−228.
Siebert, F., Mäntele, W., & Gerwert, K. (1983) *Eur. J. Biochem. 136*, 119−127.
Spurr, R. A., & Byers, H. F. (1958) *J. Phys. Chem. 62*, 425−428.
Stryer, L. (1991) *J. Biol. Chem. 266*, 10711−10714.
Tallent, J. R., Hyde, E. W., Findsen, L. A., Fox, G. C., & Birge, R. R. (1992) *J. Am. Chem. Soc. 114*, 1581−1592.
Wang, Q., Schoenlein, R. W., Peteanu, L. A., Mathies, R. A., & Shank, C. V. (1994) *Science 266*, 422−424.
Warshel, A. (1976) *Nature 260*, 679−683.
Warshel, A., Chu, Z. T., & Hwang, J.-K. (1991) *Chem. Phys. 158*, 303−314.
Yamazaki, Y., Sasaki, J., Hatanaka, M., Kandori, H., Maeda, A., Needleman, R., Shinada, T., Yoshihara, K., Brown, L. S., & Lanyi, J. K. (1995a) *Biochemistry 34*, 577−582.
Yamazaki, Y., Hatanaka, M., Kandori, H., Sasaki, J., Karstens, W. F. J., Raap, J., Lugtenburg, J., Bizounok, M., Herzfeld, J., Needleman, R., Lanyi, J. K., & Maeda, A. (1995b) *Biochemistry 34*, 7088−7093.
Yoshizawa, T., & Wald, G. (1963) *Nature 197*, 1279−1286.
Yoshizawa, T., & Kandori, H. (1992) *Prog. Retinal Res. 11*, 33−55.
Zhang, H., Lerro, K. A., Yamamoto, T., Lien, T. H., Sastry, L., Gawinowicz, M. A., & Nakanishi, K. (1994) *J. Am. Chem. Soc. 116*, 10165−10173.
Zhukovsky, E. A., & Oprian, D. D. (1989) *Science 246*, 928−930.

BI9515477